Enhanced stiffness modeling of serial manipulators with passive joints

Anatol Pashkevich[1,2], Alexandr Klimchik[1,2] and Damien Chablat[2]
[1]Ecole des Mines de Nantes
[2]Institut de Recherches en Communications et Cybernetique de Nantes
France

Abstract

The chapter focuses on the enhanced stiffness modeling and analysis of serial kinematic chains with passive joints, which are widely used in parallel robotic systems. In contrast to previous works, the stiffness is evaluated for the loaded working mode corresponding to the static equilibrium of the elastic forces and the external wrench acting upon the manipulator end point. It is assumed that the manipulator elasticity is described by a multidimensional lumped-parameter model, which consists of a chain of rigid bodies connected by 6-dof virtual springs. Each of these springs characterize flexibility of the corresponding link or actuating joint and takes into account both their translational/rotational compliance and the coupling between them. The proposed technique allows finding the full-scale "load-deflection" relation for any given workspace point and to linearise it taking into account variation of the manipulator Jacobian due to the external load. These enable evaluating critical forces that may provoke non-linear behavior of the manipulator, such as sudden failure due to elastic instability (buckling). The advantages of the developed technique are illustrated by several examples that deal with kinematic chains employed in typical parallel manipulators.

Keywords

Stiffness model, external loading, kinetostatic analysis, passive joints, buckling, divergence of equilibrium, static stability

1. Introduction

Due to the increasing industrial needs, novel approaches in mechanical design of robotic manipulators are targeted at essential reduction of moving masses and achieving high dynamic performances with relatively low energy consumption. This motivates using advanced kinematical architectures and light-weight materials, as well as minimization of the cross-sections of all manipulator elements (Siciliano & Khatib, 2008). The primary constraint for such minimization is the mechanical stiffness of the manipulator, which must be evaluated taking into account external disturbances (loading) imposed by a relevant

manufacturing process. However, in robotic literature, the manipulator stiffness is usually evaluated by a linear model, which defines the static response to the external force/torque, assuming that the compliant deflections are small and the external loading is insignificant (Zhang et al., 2009; Majou et al., 2007). At the same time, in many practical applications (such as milling, for instance), the loading is essential and conventional stiffness modeling techniques must be used with great caution (Los et al., 2008). Moreover, for the manipulators with light-weight links, there is a potential danger of buckling phenomena that is known from general theory of elastic stability (Timoshenko & Goodier, 1970). Hence, the existing stiffness modeling techniques for high-performance robotic manipulators must be revised and enhanced, in order to add ability of detecting non-linear effects and avoid structural failures caused by the loading.

The existing approaches for the manipulator stiffness modeling may be roughly divided into three main groups: the Finite Element Analysis (FEA) (Piras et al., 2005; Hu et al., 2007; Nagai & Liu 2007), the matrix structural analysis (SMA) (Deblaise et al. 2006, Martin, 1966, Li et al., 2002), and the virtual joint method (VJM) that is often called the lumped modeling (Gosselin, 1990; Pashkevich et. al. 2008; Quennouelle & Gosselin 2008 a). The most accurate of them is the Finite Element Analysis, which allows modeling links and joints with its true dimension and shape. However it is usually applied at the final design stage because of the high computational expenses required for the repeated remeshing of the complicated 3D structure over the whole workspace. The SMA also incorporates the main ideas of the FEA, but operates with rather large elements – 3D flexible beams that are presented in the manipulator structure. This leads obviously to the reduction of the computational expenses, but does not provide clear physical relations required for the parametric stiffness analysis. And finally, the VJM method is based on the expansion of the traditional rigid model by adding the virtual joints (localized springs), which describe the elastic deformations of the links, joints and actuators (Salisbury, 1980; Gosselin, 1990). The VJM technique is widely used at the pre-design stage and will be extended in this paper for the case of the preloaded manipulators.

It should be noted, that there are a number of variations and simplifications of the VJM, which differ in modeling assumptions and numerical procedures. Recent modification of this method allows to extend it to the over-constrained manipulator and to apply it at any workspace point, including the singular ones (Pashkevich et. al. 2009 a, b). Besides, to take into account real shape of the manipulator components, the stiffness parameters may be evaluated using the FEA modeling. The latter provided the FEA-accuracy throughout the whole workspace without exhaustive remeshing required for the classical FEA.

At present, there is very limited number of publication that directly addressed the problem of the stiffness modeling for loaded manipulators. The most essential results were obtained in (Alici, & Shirinzadeh; 2005; Quennouelle & Gosselin, 2008 b; Kovecses & Angeles, 2007) where the stiffness matrix was computed taking into account the change in the manipulator configuration due to the preloading. However, the problem of finding the corresponding loaded equilibrium was omitted, so the Jacobian and Hessian were computed in a traditional way, i.e. for the neighborhood of the unloaded equilibrium. The latter yielded essential computational simplification but also imposed crucial limitations, not allowing detecting the buckling and other non-liner effects.

This chapter focuses on the stiffness modeling of serial kinematic chains with passive joints, which are widely used in parallel robotic systems. It presents an enhanced solution of the

considered problem, taking into account influence of the external force/torque on the manipulator configuration as well as change in the Jacobian due to the external loading. It implements the virtual joint technique that describes the compliance of the manipulator elements by a set of localized six-dimensional springs separated by rigid links and perfect joints. In contrast to previous works, the developed technique allows to obtain the full-scale "load-deflection" relation for any given workspace point and to compute the desired matrix for any manipulator configuration (including singular ones), implicitly taking into account the kinematic redundancy imposed by the passive joints. Besides, it enables designer to evaluate critical forces that may provoke non-linear manipulator behaviour, such as sudden failure due to elastic instability (buckling) which has not been previously studied in robotic literature. Another contribution is a numerical algorithm for computing the loaded equilibrium and its analytical criteria for its stability analysis.

The remainder of the chapter is organized as follows. Section 2 defines the research problem and basic assumptions. In Section 3, it is proposed a numerical algorithm for computing of the loaded static equilibrium and its stability analysis. Section 4 focuses on the stiffness matrix evaluation taking into account external loading and presence of passive joints. Section 5 contains a set of illustrative examples that demonstrate possible nonlinear behavior of loaded serial kinematic chains. And finally, Section 6 summarizes the main results and contributions.

2. Problem of Stiffness modelling

2.1 Manipulator Architecture

Let us consider a general serial kinematic chain, which consists of a fixed "Base", a number of flexible actuated joints "Ac", a serial chain of flexible "Links", a number of passive joints "Ps" and a moving "Platform" at the end of the chain (Fig. 1). It is assumed that all links are separated by the joints (actuated or passive, rotational or translational) and the joint type order is arbitrary. Besides, it is admitted that some links may be separated by actuated and passive joints simultaneously. Such architecture can be found in most of parallel manipulators (Fig. 2) where several similar kinematic chains are connected to the same base and platform in a different way (with rotation of 90° or 120°, for instance), in order to eliminate the redundancy caused by the passive joints. It is obvious that such kinematic chains are statically *under-constrained* and their stiffness analysis can not be performed by direct application of the standard methods.

Typical examples of the examined kinematic chains can be found in 3-PUU translational parallel kinematic machine (Li & Xu, 2008), in Delta parallel robot (Clavel, 1988) or in parallel manipulators of the Orthoglide family (Chablat & Wenger, 2003) and other manipulators (Merlet, 2006). It worth mentioning that here a specific spatial arrangement of under-constrained chains yields the *over-constrained* mechanism that posses a high structural rigidity with respect to the external force. In particular, for Orthoglide, each kinematic chain prevents the platform from rotating about two orthogonal axes and any combination of two kinematic chains suppresses all possible rotations of the platform. Hence, the whole set of three kinematic chains produces non-singular stiffness matrix while for each separate chain the stiffness matrix is singular. This motivates development of dedicated stiffness analysis techniques that are presented below.
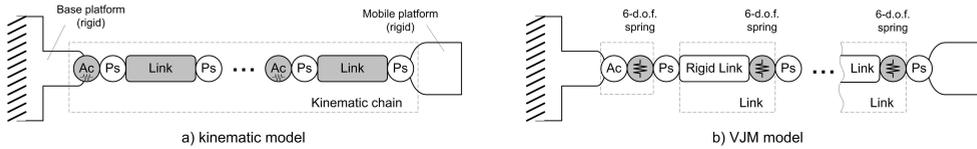
Fig. 1. General serial kinematic chain and its VJM model (Ac – actuated joint, Ps – passive joint).
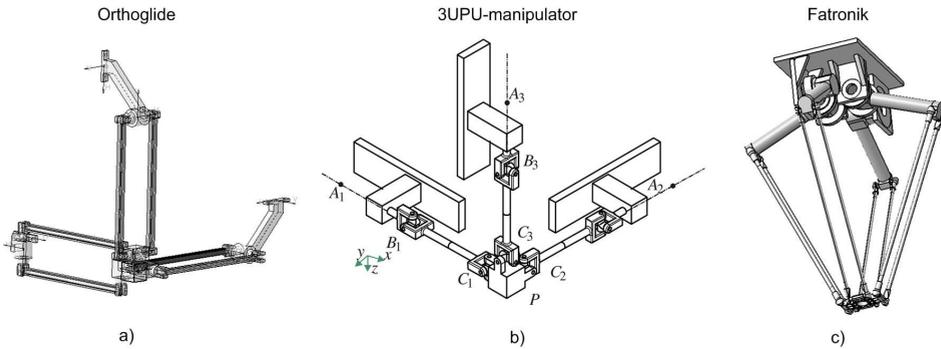
Fig. 2. Architecture of typical parallel manipulators and their kinematics chains

2.2 Basic Assumptions

To evaluate the stiffness of the considered serial manipulator, let us apply a modification of the virtual joint method (VJM), which is based on the lump modeling approach (Gosselin, 1990). According to this approach, the original rigid model should be extended by adding virtual joints (localized springs), which describe elastic deformations of the links. Besides, virtual springs are included in the actuating joints, to take into account the stiffness of the control loop. Under such assumptions, the kinematic chain can be described by the following serial structure:

(a) a rigid link between the manipulator base and the first actuating joint described by the constant homogenous transformation matrix $\mathbf{T}_{Base}$;

(b) the 6-d.o.f. actuating joints defining three translational and three rotational actuator coordinates, which are described by the homogenous matrix function $\mathbf{T}_{3D}\left(\boldsymbol{\theta}_a^i\right)$ where $\boldsymbol{\theta}_a^i = \left(\theta_x^{ai}, \theta_y^{ai}, \theta_z^{ai}, \theta_{\varphi x}^{ai}, \theta_{\varphi y}^{ai}, \theta_{\varphi z}^{ai}\right)$ are the virtual spring coordinates;

(c) the 6-d.o.f. passive joints defining three translational and three rotational passive joins coordinates, which are described by the homogenous matrix function $\mathbf{T}_{3D}\left(\mathbf{q}_p^i\right)$ where $\mathbf{q}_p^i = \left(q_x^i, q_y^i, q_z^i, q_{\varphi x}^i, q_{\varphi y}^i, q_{\varphi z}^i\right)$ are the passive joint coordinates;

(d) the rigid links, which are described by the constant homogenous transformation matrix $\mathbf{T}_{Link}^i$;

(e) a 6-d.o.f. virtual joint defining three translational and three rotational link-springs, which are described by the homogenous matrix function $\mathbf{T}_{3D}\left(\boldsymbol{\theta}_{Link}^i\right)$, where

$\boldsymbol{\theta}_{Link}^{i} = \left(\theta_{x}^{i}, \theta_{y}^{i}, \theta_{z}^{i}, \theta_{\varphi x}^{i}, \theta_{\varphi y}^{i}, \theta_{\varphi z}^{i} \right)$, $\left(\theta_{x}^{i}, \theta_{y}^{i}, \theta_{z}^{i} \right)$ and $\left(\theta_{\varphi x}^{i}, \theta_{\varphi y}^{i}, \theta_{\varphi z}^{i} \right)$ correspond to the elementary translations and rotations respectively;

(f) a rigid link from the last link to the end-effector, described by the homogenous matrix transformation $\mathbf{T}_{Tool}$.

In the frame of these notations, the final expression defining the end-effector location subject to variations of all joint coordinates of a single kinematic chain may be written as the product of the following homogenous matrices

$$\mathbf{T} = \mathbf{T}_{Base} \cdot \prod_{i} \left(\mathbf{T}_{3D}\left(\boldsymbol{\theta}_{a}^{i} \right) \cdot \mathbf{T}_{3D}\left(\mathbf{q}_{p}^{2i-1} \right) \cdot \mathbf{T}_{Link}^{i} \cdot \mathbf{T}_{3D}\left(\boldsymbol{\theta}_{Link}^{i} \right) \cdot \mathbf{T}_{3D}\left(\mathbf{q}_{p}^{2i} \right) \right) \cdot \mathbf{T}_{Tool} \tag{1}$$

where the components $\mathbf{T}_{Base}$, $\mathbf{T}_{3D}(...)$, $\mathbf{T}_{Link}^{i}$, $\mathbf{T}_{Tool}$ may be factorized with respect to the terms including the joint variables, in order to simplify computing of the derivatives (Jacobian and Hessian).

This expression includes both traditional geometric variables (passive and active joint coordinates) and stiffness variables (virtual joint coordinates). Explicit position and orientation of the end-effector can by extracted from the matrix $\mathbf{T}$ in a standard way (Angeles, 2007), so finally the kinematic model can be rewritten as the vector function

$$t = g(\mathbf{q}, \boldsymbol{\theta}) \tag{2}$$

where the vector $\mathbf{t} = (\mathbf{p}, \boldsymbol{\varphi})^{T}$ includes the position $\mathbf{p} = (x, y, z)^{T}$ and orientation $\boldsymbol{\varphi} = (\varphi_{x}, \varphi_{y}, \varphi_{z})^{T}$ of the end-platform, the vector $\mathbf{q} = (q_{1}, q_{2}, ..., q_{n})^{T}$ contains all passive joint coordinates, the vector $\boldsymbol{\theta} = (\theta_{1}, \theta_{2}, ..., \theta_{m})^{T}$ collects all virtual joint coordinates, n is the number of passive joins, m is the number of virtual joints.

2.3 Problem statement

In general, the stiffness model describes the resistance of an elastic body or a mechanism to deformations caused by an external force or torque. It can be defined by the relation $\mathbf{F} = f(\Delta \mathbf{t})$, where $f(...)$ is the function that associates a deformation $\Delta \mathbf{t}$ with an external force $\mathbf{F}$ that causes it. It worth mentioning that the function $f(...)$ can de determined even for the singular configurations (or redundant kinematics) while the inverse statement is not generally true. For relatively small deformations, this function is defined through the ''stiffness matrix'' $\mathbf{K}$, which defines the linear relation

$$\mathbf{F} = \mathbf{K}(\mathbf{q}_{0}, \boldsymbol{\theta}_{0}) \cdot \Delta \mathbf{t} \tag{3}$$

between the six-dimensional translational/rotational displacements $\Delta \mathbf{t} = (\Delta x, \Delta y, \Delta z, \Delta \varphi_{x}, \Delta \varphi_{y}, \Delta \varphi_{z})^{T}$, and the static forces/torques $\mathbf{F} = \left(F_{x}, F_{y}, F_{z}, M_{x}, M_{y}, M_{z} \right)$ causing this transition. Here, the vector $\mathbf{q}_{0} = (q_{01}, q_{02}, ..., q_{0n})^{T}$ includes all passive joint coordinates, the vector $\boldsymbol{\theta}_{0} = (\theta_{01}, \theta_{02}, ..., \theta_{0m})^{T}$ collects all virtual joint coordinates, n is the

number of passive joins, m is the number of virtual joints. Usually, the manipulator is assembled without internal preloading, so the vector $\mathbf{\theta}_0$ is equal to zero.

However, for the loaded mode, similar relation is defined in the neighborhood of another static equilibrium, which corresponds to a different manipulator configuration $(\mathbf{q}, \mathbf{\theta})$, that is caused by external forces/torques $\mathbf{F}$. Respectively, in this case, the stiffness model describes the relation between the increments of the force $\mathbf{\delta F}$ and the position $\mathbf{\delta t}$

$$\mathbf{\delta F} = \mathbf{K}^F(\mathbf{q}, \mathbf{\theta}) \cdot \mathbf{\delta t} \tag{4}$$

where $\mathbf{q} = \mathbf{q_0} + \mathbf{\Delta q}$ and $\mathbf{\theta} = \mathbf{\theta_0} + \mathbf{\Delta\theta}$ denote the new configuration of the manipulator, and $\mathbf{\Delta q}$, $\mathbf{\Delta\theta}$ are the deviations of the passive joint and virtual spring coordinates respectively.

Hence, the considered problem may be divided into three sequential subtasks: (i) finding the static equilibrium for the loaded configuration and checking its stability, (ii) linearization of the relevant force/position relations in the neighborhood of this equilibrium, and finally (iii) determining the critical force for the kinematic chain that may cause undesired buckling phenomena.

3. Static equilibrium for loaded mode

Computing of the static equilibrium is a key issue for the stiffness analysis, since it defines the manipulator configuration $(\mathbf{q}, \mathbf{\theta})$ required for the linearization of the "load-deflection" relation. In previous works, this issue was usually ignored and the linearization was performed in the neighborhood of the unloaded configuration assuming that the external load is small enough. It is obvious that the latter essentially limits relevant results and do not allow to detect non-linear effects such as the buckling. From mathematical point of view, the problem is reduced to finding solutions of a system of non-linear equations that may be unique or non-unique, stable or unstable.

3.1 Configuration of loaded manipulator

Let us assume that, due to the external force $\mathbf{F}$, the end-effector of the manipulator is relocated from the initial (unloaded) position $\mathbf{t}_0 = g(\mathbf{q}_0, \mathbf{\theta}_0)$ to a new position $\mathbf{t} = g(\mathbf{q}, \mathbf{\theta})$, which satisfies the condition of the mechanical equilibrium. Here $\mathbf{q}_0$ is computed via the inverse kinematics and $\mathbf{\theta}_0$ is equal to zero (since there are no external loading in the springs), $\mathbf{q}, \mathbf{\theta}$ are passive and virtual joint coordinate in the loaded mode respectively. For rather small displacement $\mathbf{\Delta t} = \mathbf{t} - \mathbf{t}_0$, a new position of the end-effector $\mathbf{t} = P(\mathbf{q}_0 + \mathbf{\Delta q}, \mathbf{\theta}_0 + \mathbf{\Delta\theta})$ may be expressed as

$$\mathbf{t} = \mathbf{t}_0 + \mathbf{J}_\theta \cdot \mathbf{\Delta\theta} + \mathbf{J}_q \cdot \mathbf{\Delta q} \tag{5}$$

where $\mathbf{J}_\theta$ and $\mathbf{J}_q$ are the kinematic Jacobians with respect to the coordinates $\mathbf{\theta}$, $\mathbf{q}$, which may be computed from (1), (2) analytically or semi-analytically, using the factorization

technique. However, in general case, the model is highly non-linear and computing $\mathbf{J}_\theta$ and $\mathbf{J}_q$ requires some additional efforts.

For computational reasons, let us consider the dual problem that deals with determining the external force $\mathbf{F}$ and the manipulator configuration $(\mathbf{q}, \boldsymbol{\theta})$ that correspond to the output position $\mathbf{t}$.

Let us assume that the joints are given small, arbitrary virtual displacements $\delta \mathbf{q}, \delta \boldsymbol{\theta}$ in the equilibrium neighborhood.

According to the principle of virtual displacements, the virtual work of the external force $\mathbf{F}$ applied to the end-effector along the corresponding displacement $\delta \mathbf{t} = \mathbf{J}_\theta \cdot \delta \boldsymbol{\theta} + \mathbf{J}_q \cdot \delta \mathbf{q}$ is equal to the sum $\left(\mathbf{F}^T \mathbf{J}_\theta \right) \cdot \delta \boldsymbol{\theta} + \left(\mathbf{F}^T \mathbf{J}_q \right) \cdot \delta \mathbf{q}$. Since the passive joints do not produce the force/torque reactions, the virtual work includes only one component $-\boldsymbol{\tau}_\theta^{\ T} \cdot \delta \boldsymbol{\theta}$ (the minus sign takes into account the force-displacement directions for the virtual spring). In the static equilibrium, the total virtual work of all forces is equal to zero for any virtual displacement, therefore the equilibrium conditions may be written as

$$\mathbf{J}_\theta^{\ T} \cdot \mathbf{F} = \boldsymbol{\tau}_\theta; \qquad \mathbf{J}_q^{\ T} \cdot \mathbf{F} = \mathbf{0} \tag{6}$$

Taking into account (3), the latter system of equations can be rewritten as

$$\mathbf{F}^T \cdot \mathbf{J}_\theta = \mathbf{K}_\theta \cdot \boldsymbol{\theta}; \qquad \mathbf{F}^T \cdot \mathbf{J}_q = 0 \tag{7}$$

It is evident that there is no general method for analytical solution of this system and it is required to apply numerical techniques. To derive the numerical algorithm, let us linearize the kinematic equation in the neighborhood of the current position $(\mathbf{q}_i, \boldsymbol{\theta}_i)$

$$\mathbf{t} = P(\mathbf{q}_i, \boldsymbol{\theta}_i) + \mathbf{J}_q(\mathbf{q}_i, \boldsymbol{\theta}_i) \cdot (\mathbf{q}_{i+1} - \mathbf{q}_i) + \mathbf{J}_\theta(\mathbf{q}_i, \boldsymbol{\theta}_i) \cdot (\boldsymbol{\theta}_{i+1} - \boldsymbol{\theta}_i) \tag{8}$$

and rewrite the static equilibrium equations as

$$\mathbf{J}_\theta^{\ T}(\mathbf{q}_i, \boldsymbol{\theta}_i) \cdot \mathbf{F}_{i+1} = \mathbf{K}_\theta \, \boldsymbol{\theta}_{i+1}; \qquad \mathbf{J}_q^{\ T}(\mathbf{q}_i, \boldsymbol{\theta}_i) \cdot \mathbf{F}_{i+1} = \mathbf{0} \tag{9}$$

This leads to a linear algebraic system of equations with respect to $(\mathbf{q}_{i+1}, \boldsymbol{\theta}_{i+1}, \mathbf{F}_{i+1})$

$$\mathbf{J}_q(\mathbf{q}_i, \boldsymbol{\theta}_i) \cdot \mathbf{q}_{i+1} + \mathbf{J}_\theta(\mathbf{q}_i, \boldsymbol{\theta}_i) \cdot \boldsymbol{\theta}_{i+1} = \mathbf{t} - \mathbf{f}(\mathbf{q}_i, \boldsymbol{\theta}_i) + \mathbf{J}_q(\mathbf{q}_i, \boldsymbol{\theta}_i) \cdot \mathbf{q}_i + \mathbf{J}_\theta(\mathbf{q}_i, \boldsymbol{\theta}_i) \cdot \boldsymbol{\theta}_i$$
$$-\mathbf{K}_\theta \cdot \boldsymbol{\theta}_{i+1} + \mathbf{J}_\theta^{\ T}(\mathbf{q}_i, \boldsymbol{\theta}_i) \cdot \mathbf{F}_{i+1} = \mathbf{0} \tag{10}$$
$$\mathbf{J}_q^{\ T}(\mathbf{q}_i, \boldsymbol{\theta}_i) \cdot \mathbf{F}_{i+1} = \mathbf{0}$$

which gives the following iterative scheme

$$\begin{bmatrix} \mathbf{F}_{i+1} \\ \mathbf{q}_{i+1} \end{bmatrix} = \begin{bmatrix} \mathbf{J}_{\theta}(\mathbf{q}_i, \boldsymbol{\theta}_i) \mathbf{K}_{\theta}^{-1} \mathbf{J}_{\theta}^{T}(\mathbf{q}_i, \boldsymbol{\theta}_i) & \mathbf{J}_q(\mathbf{q}_i, \boldsymbol{\theta}_i) \\ \mathbf{J}_q^{T}(\mathbf{q}_i, \boldsymbol{\theta}_i) & 0 \end{bmatrix}^{-1} \begin{bmatrix} \mathbf{t} - \mathbf{f}(\mathbf{q}_i, \boldsymbol{\theta}_i) + \mathbf{J}_q(\mathbf{q}_i, \boldsymbol{\theta}_i) \mathbf{q}_i + \mathbf{J}_{\theta}(\mathbf{q}_i, \boldsymbol{\theta}_i) \boldsymbol{\theta}_i \\ 0 \end{bmatrix} \quad (11)$$

$$\boldsymbol{\theta}_{i+1} = \mathbf{K}_{\theta}^{-1} \cdot \mathbf{J}_{\theta}^{T}(\mathbf{q}_i, \boldsymbol{\theta}_i) \cdot \mathbf{F}_{i+1}$$

where the starting point $(\mathbf{q}_0, \boldsymbol{\theta}_0)$ can be chosen using the non-loaded configuration, and computed via the inverse kinematics.

As follows from computational experiments, for typical values of deformations the proposed iterative algorithm possesses rather good convergence (3-5 iterations are usually enough). However, in the case of buckling or in the area of multiple equilibriums, the problem of convergence becomes rather critical and highly depends on the initial guess. To overcome this problem, the value of the joint variables $(\boldsymbol{\theta}_i, \mathbf{q}_i)$ computed at each iteration were disturbed by adding small random noise. Further enhancement of this algorithm may be based on the full-scale Newton-Raphson technique (i.e. linearization of the static equilibrium equations in addition to the kinematic one), this obviously increases computational expenses but potentially improves convergence.

3.2 Stability of the static equilibrium

To evaluate stability of the computed static equilibrium $(\mathbf{q}, \boldsymbol{\theta})$, let us assume that the manipulator end-effector is fixed at the point $\mathbf{p}$ corresponding to the external load $\mathbf{F}$, but the joint coordinates are given small virtual displacements $\delta\mathbf{q}$, $\delta\boldsymbol{\theta}$ satisfying the geometrical constraint (2), i.e.

$$\mathbf{p} = \mathbf{g}(\mathbf{q}, \boldsymbol{\theta}); \qquad \mathbf{p} = \mathbf{g}(\mathbf{q} + \delta\mathbf{q}, \boldsymbol{\theta} + \delta\boldsymbol{\theta}) \qquad (12)$$

For these assumptions, let us compute the total virtual work in the joints that must be positive for a stable equilibrium and negative for an unstable one.

To achieve the virtual configuration $(\mathbf{q} + \delta\mathbf{q}, \boldsymbol{\theta} + \delta\boldsymbol{\theta})$ and restore the equilibrium conditions, each of the joints must include virtual motors that generate the generalized forces/torques $\delta\boldsymbol{\tau}_q$, $\delta\boldsymbol{\tau}_{\theta}$ which satisfies the equations:

$$\begin{aligned} \mathbf{J}_{\theta}^{T} \mathbf{F} &= \mathbf{K}_{\theta} \boldsymbol{\theta}; & (\mathbf{J}_{\theta} + \delta\mathbf{J}_{\theta})^{T} \mathbf{F} &= \mathbf{K}_{\theta}(\boldsymbol{\theta} + \delta\boldsymbol{\theta}) + \delta\boldsymbol{\tau}_{\theta} \\ \mathbf{J}_q^{T} \mathbf{F} &= 0; & (\mathbf{J}_q + \delta\mathbf{J}_q)^{T} \mathbf{F} &= \delta\boldsymbol{\tau}_q \end{aligned} \qquad (13)$$

After relevant transformations, the virtual torques may be expressed as

$$\delta\boldsymbol{\tau}_{\theta} = \delta(\mathbf{J}_{\theta}^{T} \mathbf{F}) - \mathbf{K}_{\theta} \delta\boldsymbol{\theta}; \qquad \delta\boldsymbol{\tau}_q = \delta(\mathbf{J}_q^{T} \mathbf{F}) \qquad (14)$$

where $\delta(.)$ denotes the differential with respect to $\delta\mathbf{q}$, $\delta\boldsymbol{\theta}$ that may be expanded via the Hessians of the scalar function $\Psi = \mathbf{g}(\mathbf{q}, \boldsymbol{\theta})^{T} \mathbf{F}$:

$$\delta(\mathbf{J}_\theta^T \mathbf{F}) = \mathbf{H}_{\theta q}^F \, \delta\mathbf{q} + \mathbf{H}_{\theta\theta}^F \, \delta\mathbf{\theta}; \qquad \delta(\mathbf{J}_q^T \mathbf{F}) = \mathbf{H}_{qq}^F \, \delta\mathbf{q} + \mathbf{H}_{q\theta}^F \, \delta\mathbf{\theta} \tag{15}$$

provided that

$$\mathbf{H}_{qq}^F = \partial^2 \Psi / \partial \mathbf{q}^2; \qquad \mathbf{H}_{\theta\theta}^F = \partial^2 \Psi / \partial \mathbf{\theta}^2; \qquad \mathbf{H}_{q\theta}^F = \mathbf{H}_{\theta q}^F = \partial^2 \Psi / \partial \mathbf{q} \, \partial \mathbf{\theta} \tag{16}$$

Further, taking into account that the virtual displacement from $(\mathbf{q}, \mathbf{\theta})$ to $(\mathbf{q} + \delta\mathbf{q}, \mathbf{\theta} + \delta\mathbf{\theta})$ leads to a gradual change of the virtual torques from $(\mathbf{0}, \mathbf{0})$ to $(\delta\mathbf{\tau}_q, \delta\mathbf{\tau}_\theta)$, the virtual work may be computed as a half of the corresponding scalar products

$$\delta W = -\frac{1}{2}\left(\delta\mathbf{\tau}_\theta^T \, \delta\mathbf{\theta} + \delta\mathbf{\tau}_q^T \, \delta\mathbf{q}\right), \tag{17}$$

where the minus sign takes into account the adopted conventions for the positive directions of the forces and displacements. Hence, after appropriate substitutions and transforming to the matrix form, the desired stability condition may be written as

$$\delta W = -\frac{1}{2}\begin{bmatrix} \delta\mathbf{\theta}^T & \delta\mathbf{q}^T \end{bmatrix} \begin{bmatrix} \mathbf{H}_{\theta\theta}^F - \mathbf{K}_\theta & \mathbf{H}_{q\theta}^F \\ \mathbf{H}_{\theta q}^F & \mathbf{H}_{qq}^F \end{bmatrix} \begin{bmatrix} \delta\mathbf{\theta} \\ \delta\mathbf{q} \end{bmatrix} > 0 \tag{18}$$

where $\delta\mathbf{q}$ and $\delta\mathbf{\theta}$ must satisfy to the geometrical constraints (12).
In order to take into account the relation between $\delta\mathbf{q}$ and $\delta\mathbf{\theta}$ that is imposed by (12), let us apply the first-order expansion of the function $\mathbf{g}(\mathbf{\theta}, \mathbf{q})$ that yields the following linear relation

$$\begin{bmatrix} \mathbf{J}_\theta & \mathbf{J}_q \end{bmatrix} \cdot \begin{bmatrix} \delta\mathbf{\theta} \\ \delta\mathbf{q} \end{bmatrix} = \mathbf{0} . \tag{19}$$

Then, applying the SVD- factorization (Strang, 1998) of the integrated Jacobian

$$\begin{bmatrix} \mathbf{J}_\theta & \mathbf{J}_q \end{bmatrix} = \begin{bmatrix} \mathbf{U}_\theta & \mathbf{U}_q \end{bmatrix} \cdot \begin{bmatrix} \mathbf{S}_r & \\ & \mathbf{0} \end{bmatrix} \begin{bmatrix} \mathbf{V}_\theta^T \\ \mathbf{V}_q^T \end{bmatrix} \tag{20}$$

and extracting from $\mathbf{V}_\theta$, $\mathbf{V}_q$ the sub-matrices $\mathbf{V}_\theta^o$, $\mathbf{V}_q^o$ corresponding to the zero singular values, a relevant null-space of the system (19) may be presented as

$$\delta\mathbf{\theta} = \mathbf{V}_\theta^o \cdot \delta\mathbf{\mu}; \qquad \delta\mathbf{q} = \mathbf{V}_q^o \cdot \delta\mathbf{\mu} \tag{21}$$

where $\delta\mathbf{\mu}$ is the arbitrary vector of the appropriate dimension (equal to the rank-deficiency of the Integrated Jacobian). Hence, the stability condition (18) may be rewritten as inequality

$$\delta W = -\frac{1}{2} \delta \boldsymbol{\mu}^T \cdot \begin{bmatrix} \mathbf{V}_\theta^o \\ \mathbf{V}_q^o \end{bmatrix}^T \cdot \begin{bmatrix} \mathbf{H}_{\theta\theta}^F - \mathbf{K}_\theta & \mathbf{H}_{q\theta}^F \\ \mathbf{H}_{\theta q}^F & \mathbf{H}_{qq}^F \end{bmatrix} \cdot \begin{bmatrix} \mathbf{V}_\theta^o \\ \mathbf{V}_\theta^o \end{bmatrix} \cdot \delta \boldsymbol{\mu} > 0 \qquad (22)$$

that must be satisfied for all non-zero $\delta \boldsymbol{\mu}$. In other words, the considered static equilibrium $(\mathbf{q}, \boldsymbol{\theta})$ is stable if (and only if) the matrix

$$\begin{bmatrix} \mathbf{V}_\theta^o \\ \mathbf{V}_q^o \end{bmatrix}^T \cdot \begin{bmatrix} \mathbf{H}_{\theta\theta}^F - \mathbf{K}_\theta & \mathbf{H}_{q\theta}^F \\ \mathbf{H}_{\theta q}^F & \mathbf{H}_{qq}^F \end{bmatrix} \cdot \begin{bmatrix} \mathbf{V}_\theta^o \\ \mathbf{V}_\theta^o \end{bmatrix} < 0 \qquad (23)$$

is positive-negative. It is worth mentioning that the obtained result is in a good agreement with previous studies (Alici & Shirinzadeh, 2005), where (for manipulators without passive joints) the stiffness properties were defined by the matrix $\mathbf{K}_\theta - \mathbf{H}_{\theta\theta}^F$ that must be positive-definite.

4. Stiffness model for the loaded mode

The previous section presents a technique that allows obtaining an exact relation between the elastic deformations and corresponding external force/torque. It is based on sequential computations of loaded equilibriums (and relevant force/torque) for various displacements of the manipulator end-point with respect to its unloaded location. However, in general case, this relation is highly non-linear while common engineering practice operates with the stiffness matrix derived via the linearization.

To compute the desired stiffness matrix, let us consider the neighborhood of the loaded configuration and assume that the external force and the end-effector location are incremented by some small values $\delta \mathbf{F}$, $\delta \mathbf{t}$. Besides, let us assume that a new configuration also satisfies the equilibrium conditions. Hence, it is necessary to consider simultaneously two equilibriums corresponding to the manipulator state variables $(\mathbf{F}, \mathbf{q}, \boldsymbol{\theta}, \mathbf{t})$ and $(\mathbf{F} + \delta \mathbf{F}, \mathbf{q} + \delta \mathbf{q}, \boldsymbol{\theta} + \delta \boldsymbol{\theta}, \mathbf{t} + \delta \mathbf{t})$. Relevant equations of statics may be written as

$$\mathbf{F} \cdot \mathbf{J}_\theta^T = \mathbf{K}_\theta \cdot \boldsymbol{\theta}; \qquad \mathbf{F} \cdot \mathbf{J}_q^T = 0 \qquad (24)$$

and

$$(\mathbf{F} + \delta \mathbf{F}) \cdot (\mathbf{J}_\theta + \delta \mathbf{J}_\theta)^T = \mathbf{K}_\theta \cdot (\boldsymbol{\theta} + \delta \boldsymbol{\theta});$$
$$(\mathbf{F} + \delta \mathbf{F}) \cdot (\mathbf{J}_q + \delta \mathbf{J}_q)^T = 0 \qquad (25)$$

where $\delta \mathbf{J}_q(\mathbf{q}, \boldsymbol{\theta})$ and $\delta \mathbf{J}_\theta(\mathbf{q}, \boldsymbol{\theta})$ are the differentials of the Jacobians due to changes in $(\mathbf{q}, \boldsymbol{\theta})$. Besides, in the neighborhood of $(\mathbf{q}, \boldsymbol{\theta})$, the kinematic equation may be also presented in the linearized form:

$$\delta \mathbf{t} = \mathbf{J}_\theta(\mathbf{q}, \boldsymbol{\theta}) \cdot \delta \boldsymbol{\theta} + \mathbf{J}_q(\mathbf{q}, \boldsymbol{\theta}) \cdot \delta \mathbf{q} \, , \tag{26}$$

Hence, after neglecting the high-order small terms and expending the differentials via the Hessians of the function $\Psi = \mathbf{g}(\mathbf{q}, \boldsymbol{\theta})^T \mathbf{F}$ (similar to sub-section 3.2), equations (24), (25) may be rewritten as

$$\mathbf{J}_\theta{}^T(\mathbf{q}, \boldsymbol{\theta}) \cdot \delta \mathbf{F} + \mathbf{H}_{\theta q}^F(\mathbf{q}, \boldsymbol{\theta}) \cdot \delta \mathbf{q} + \mathbf{H}_{\theta \theta}^F(\mathbf{q}, \boldsymbol{\theta}) \cdot \delta \boldsymbol{\theta} = \mathbf{K}_\theta \cdot \delta \boldsymbol{\theta}$$

$$\mathbf{J}_q{}^T(\mathbf{q}, \boldsymbol{\theta}) \cdot \delta \mathbf{F} + \mathbf{H}_{qq}^F(\mathbf{q}, \boldsymbol{\theta}) \cdot \delta \mathbf{q} + \mathbf{H}_{q\theta}^F(\mathbf{q}, \boldsymbol{\theta}) \cdot \delta \boldsymbol{\theta} = \mathbf{0} \tag{27}$$

and the general relation between the increments $\delta \mathbf{F}$, $\delta \mathbf{t}$, $\delta \boldsymbol{\theta}$, $\delta \mathbf{q}$ can be presented as

$$\begin{bmatrix} \mathbf{0} & \mathbf{J}_q & \mathbf{J}_\theta \\ \mathbf{J}_q^T & \mathbf{H}_{\theta\theta}^F - \mathbf{K}_\theta & \mathbf{H}_{\theta q}^F \\ \mathbf{J}_\theta^T & \mathbf{H}_{q\theta}^F & \mathbf{H}_{qq}^F \end{bmatrix} \cdot \begin{bmatrix} \delta \mathbf{F} \\ \delta \boldsymbol{\theta} \\ \delta \mathbf{q} \end{bmatrix} = \begin{bmatrix} \delta \mathbf{t} \\ \mathbf{0} \\ \mathbf{0} \end{bmatrix} . \tag{28}$$

The latter gives a straightforward numerical technique for computing of the desired stiffness matrix: direct inversion of the matrix in the left-hand side of (28) and extracting from it the upper-left sub-matrix of size 6×6. Similarly, there can be computed the matrices defining linear relations between the end-effector increment $\delta \mathbf{t}$ and the increments of the joint variables $\delta \boldsymbol{\theta}$, $\delta \mathbf{q}$, i.e.:

$$\delta \mathbf{F} = \mathbf{K}_F \cdot \delta \mathbf{t}; \qquad \delta \boldsymbol{\theta} = \mathbf{K}_\theta \cdot \delta \mathbf{t}; \qquad \delta \mathbf{q} = \mathbf{K}_q \cdot \delta \mathbf{t} \tag{29}$$

where

$$\begin{bmatrix} \mathbf{0} & \mathbf{J}_q & \mathbf{J}_\theta \\ \mathbf{J}_q^T & \mathbf{H}_{\theta\theta}^F - \mathbf{K}_\theta & \mathbf{H}_{\theta q}^F \\ \mathbf{J}_\theta^T & \mathbf{H}_{q\theta}^F & \mathbf{H}_{qq}^F \end{bmatrix}^{-1} = \begin{bmatrix} \mathbf{K}_F & \vdots & \mathbf{K}_\theta & \vdots & \mathbf{K}_q \\ \hline * & \vdots & * & \vdots & * \\ \hline * & \vdots & * & \vdots & * \end{bmatrix} \tag{30}$$

In the case when the above matrix inverse is computationally hard, the variable $\delta \boldsymbol{\theta}$ can be eliminated analytically, using corresponding static equation: $\delta \boldsymbol{\theta} = \mathbf{k}_\theta^F \mathbf{J}_\theta^T \cdot \delta \mathbf{F} + \mathbf{k}_\theta^F \mathbf{H}_{\theta q}^F \cdot \delta \mathbf{q}$, .

where $\mathbf{k}_\theta^F = \left(\mathbf{K}_\theta - \mathbf{H}_{\theta\theta}^F \right)^{-1}$. This leads to a reduced system of matrix equations with unknowns $\delta \mathbf{F}$ and $\delta \mathbf{q}$

$$\begin{bmatrix} \mathbf{J}_\theta \cdot \mathbf{k}_\theta^F \cdot \mathbf{J}_\theta{}^T & \mathbf{J}_q + \mathbf{J}_\theta \cdot \mathbf{k}_\theta^F \cdot \mathbf{H}_{\theta q}^F \\ \mathbf{J}_q{}^T + \mathbf{H}_{q\theta}^F \cdot \mathbf{k}_\theta^F \cdot \mathbf{J}_\theta{}^T & \mathbf{H}_{qq}^F + \mathbf{H}_{q\theta}^F \cdot \mathbf{k}_\theta^F \cdot \mathbf{H}_{\theta q}^F \end{bmatrix} \cdot \begin{bmatrix} \delta \mathbf{F} \\ \delta \mathbf{q} \end{bmatrix} = \begin{bmatrix} \delta \mathbf{t} \\ \mathbf{0} \end{bmatrix} . \tag{31}$$

that may be treated in the similar way, i.e. the desired stiffness matrix is also obtained by direct inversion of the matrix in the left-hand side of (31) and extracting from it the upper-left sub-matrix of size 6×6:

$$\begin{bmatrix} \mathbf{J}_\theta \mathbf{k}_\theta^F \mathbf{J}_\theta^T & \mathbf{J}_q + \mathbf{J}_\theta \mathbf{k}_\theta^F \mathbf{H}_{\theta q}^F \\ \mathbf{J}_q^T + \mathbf{H}_{q\theta}^F \mathbf{k}_\theta^F \mathbf{J}_\theta^T & \mathbf{H}_{qq}^F + \mathbf{H}_{q\theta}^F \mathbf{k}_\theta^F \mathbf{H}_{\theta q}^F \end{bmatrix}^{-1} = \begin{bmatrix} \mathbf{K}_F & \vdots & \mathbf{K}_q \\ \ast & \vdots & \ast \end{bmatrix} \tag{32}$$

It worth mentioning that the structure of the latter matrix is similar to one obtained for the unloaded manipulator in (Pashkevich et al., 2009 c) and differs only by Hessians that take into account influence of the external load. It should be also noted that, because of presence of the passive joints, the stiffness matrix of a separate serial kinematic chain is always singular, but aggregation of all the manipulator chains of a parallel manipulator produce a non-singular stiffness matrix.

Hence, the presented technique allows computing the stiffness matrix in the presence of the external load and to generalize previous results both for serial kinematic chains and for parallel manipulators. It the following Section, it will be applied to several examples that deal with kinematic chains employed in typical parallel manipulators.

5. Illustrative examples

Let us apply the developed technique to the stiffness analysis of a serial kinematic chain consisting of three similar links separated by two similar rotating actuated joints. It is assumed that the chain is a part of a parallel manipulator and it is connected to the robot base via a universal passive joint and the end-platform connection is achieved via a spherical passive joint. In order to investigate possible non-linear effects in the stiffness behavior of such architecture, let us consider several cases that differ in stiffness models of the links and actuated joints.

5.1 Examined models

5.1.1 Manipulator geometry

In general, the geometry of the examined kinematic chain (Fig. 2) can be defined as $U_p R_a R_a S_p$ where R, U and S denote respectively the rotational, universal and spherical joints, and the subscripts 'p' and 'a' refer to passive and active joints respectively. Using the homogenous matrix transformations, the chain geometry may be described by the equation

$$\mathbf{T} = \mathbf{R}_u(\mathbf{q}_0) \cdot \mathbf{T}_x(L) \cdot \mathbf{T}_s(\boldsymbol{\theta}_1) \cdot \mathbf{R}_z(q_{a1}) \cdot \mathbf{T}_x(L) \cdot \mathbf{T}_s(\boldsymbol{\theta}_2) \cdot \mathbf{R}_z(q_{a2}) \cdot \mathbf{T}_x(L) \cdot \mathbf{T}_s(\boldsymbol{\theta}_3) \cdot \mathbf{R}_s(\mathbf{q}_t) \tag{33}$$

where $\mathbf{R}_z(...)$ and $\mathbf{T}_x(...)$ are the elementary rotation/translation matrices around/along the z- and x-axes, $\mathbf{R}_u(...)$ is the homogeneous rotation matrix of the universal joint (incorporating two elementary rotations), $\mathbf{R}_s(.)$ is the homogeneous rotation matrix of the universal joint (incorporating three elementary rotations), q_{a1}, q_{a2} are the coordinates of the actuated joints, L is the length of the links, $\mathbf{q}_0$ is the coordinate vector of the universal passive joint located at the robot base, $\mathbf{q}_t$ is the coordinate vector corresponding to the passive spherical joint at the end-platform, $\mathbf{T}_s(.)$ is the homogenous vector-function describing elastic deformations in the links and actuators (they are represented by the virtual coordinates incorporated in the vectors $\boldsymbol{\theta}_1, \boldsymbol{\theta}_2, \boldsymbol{\theta}_3$). It is obvious that this model can

be easily transformed into the form $\mathbf{t} = \mathbf{g}(\mathbf{q}, \boldsymbol{\theta})$ used in the frame of the developed technique.

a) **S-configuration**   b) **Π-configuration**   c) **Z-configuration**
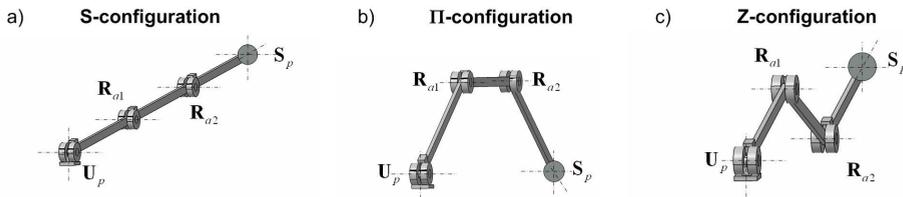
Fig. 3. Examined kinematical chain and its typical configurations (Up – passive universal joint, Ra1, Ra2 – actuated rotating joints, Sp – passive spherical joint)

To investigate particularities of this architecture, let us also define three typical postures that differ in values of the actuated coordinates:

> *S-configuration: the links are located along the straight line (Fig. 2a),*
> *the actuated coordinates are* $q_{a1} = q_{q2} = 0$
>
> *Π-configuration: the chain takes a trapezoid shape (Fig. 2b),*
> *the actuated coordinates are* $q_{a1} = q_{q2} = -30°$
>
> *Z-configuration: the chain takes a zig-zag shape (Fig. 2c),*
> *the actuated coordinates are* $q_{a1} = -q_{q2} = 30°$

For presentational convenience, let us also assume that the coordinates $\mathbf{q}_0$ of the universal passive joint are computed to ensure location of the end-effector on the Cartesian axis x.

For each of these configurations, let us consider three types of the virtual springs corresponding to different physical assumptions concerning the stiffness properties of the actuators/links. They cover the cases, in which the main flexibility is caused by the torsion in the actuators, by the link bending, and by the combination of elementary deformations of the links.

5.1.2 Case of 1D-springs: Model A

Here, it is assumed that the flexible elements are localized in the actuating drives while the links are considered as strictly rigid. It allows, without loss of generality, to reduce the original $U_pR_aR_aS_p$ model down to $R_pR_aR_aR_p$ and define a single stiffness parameter K_θ (similar for both actuators) that will be used as a reference value for the further analysis. Besides, it is possible to ignore the end-effector orientation and consider a single passive joint coordinate q (at the base) and two virtual joint coordinates θ_1, θ_2 (at actuators). This restricts the end-effector motions to Cartesian xy-plane where the geometrical model is defined by equations

$$
\begin{aligned}
x &= L \cdot \cos q + L \cdot \cos q_{12} + L \cdot \cos q_{13}, \\
y &= L \cdot \sin q + L \cdot \sin q_{12} + L \cdot \sin q_{13}
\end{aligned}
\tag{34}
$$

where $q_{12} = q + \theta_1$ and $q_{13} = q + \theta_1 + \theta_2$. In this case, the Jacobian matrices are also computed easily

$$\mathbf{J}_q = L \cdot \begin{bmatrix} -\sin q - \sin q_{12} - \sin q_{13} \\ \cos q + \cos q_{12} + \cos q_{13} \end{bmatrix}; \quad \mathbf{J}_\theta = L \cdot \begin{bmatrix} -\sin q_{12} - \sin q_{13} & -\sin q_{13} \\ \cos q_{12} + \cos q_{13} & \cos q_{13} \end{bmatrix} \quad (35)$$

and corresponding stiffness analysis will be performed analytically and compared with numerical results that were obtained using the developed methodology.

5.1.3 Case of 2D springs: Model B

For this model, let us assume that the actuators do not include flexible components but the manipulator links are subject to non-negligible deformations in Cartesian xy-plane (bending and compression). Correspondingly, the link flexibility is defined by a 3×3 matrix that includes elements describing deformation in x- and y- directions and rotational deformation with respect to z-axis. Relevant stiffness matrix may be written as (Connor, 1976)

$$\mathbf{K} = \frac{E}{L^3} \cdot \begin{bmatrix} A \cdot L^2 & 0 & 0 \\ 0 & 12 \cdot I & -6 \cdot I \cdot L \\ 0 & -6 \cdot I \cdot L & 4 \cdot I \cdot L^2 \end{bmatrix} \quad (36)$$

where L is the length of the links, I and A are respectively its second moment and area of the cross-section , and E is the Young module. Further, for comparison purposes, let us re-parameterize this matrix K to be closer to model A. In particular, let us denote the element $k_{3,3}$ (corresponding to z-rotation) of the compliant matrix $\mathbf{k} = \mathbf{K}^{-1}$ as $1/K_\theta$ and eliminate the Young module. This yields expression

$$\mathbf{k} = \frac{1}{K_\theta} \cdot \begin{bmatrix} I/A & 0 & 0 \\ 0 & L^2/3 & L/2 \\ 0 & L/2 & 1 \end{bmatrix} \quad (37)$$

where, for a rectangular cross-section $a \times b$, the required parameters may be computed as $A = ab$ and $I = ab^3/12$.

From kinematical point of view, model B is also restricted to Cartesian xy-plane and is described by the expression $R_pR_aR_aR_p$. However, in addition to a single passive joint coordinate q , here there are nine coordinates of the virtual spring (three for each link). The kinematic model of this manipulator is defined by equations

$$\begin{aligned} x &= L_1 \cdot \cos q + L_2 \cdot \cos q_{12} + \theta_2 \cdot \sin q_{12} + L_3 \cdot \cos q_{13} + \theta_5 \cdot \sin q_{13} + L_4 \cdot \cos q_{14} + \theta_8 \cdot \sin q_{14}, \\ y &= L_1 \cdot \sin q + L_2 \cdot \sin q_{12} + \theta_2 \cdot \cos q_{12} + L_3 \cdot \sin q_{13} + \theta_5 \cdot \cos q_{13} + L_4 \cdot \sin q_{14} + \theta_8 \cdot \cos q_{14} \end{aligned} \quad (38)$$

where $L_1 = L$, $L_2 = L + \theta_1$, $L_3 = L + \theta_4$, $L_4 = \theta_7$, $q_{12} = q + \theta_3$, $q_{13} = q + \theta_3 + \theta_6$, $q_{14} = q + \theta_3 + \theta_6 + \theta_9$, and $\boldsymbol{\theta}_1 = (\theta_1, \theta_2, \theta_3)$, $\boldsymbol{\theta}_2 = (\theta_4, \theta_5, \theta_6)$, $\boldsymbol{\theta}_3 = (\theta_7, \theta_8, \theta_9)$ are the spring joint coordinates for the first, second and third links respectively. The Jacobian matrices in this case can be also computed analytically but their dimensions are too high for analytical computations. Hence, in this case this stiffness analysis will be performed numerically.

5.1.4 Case of 3D springs: Model C

This case also assumes that that the actuators are strictly rigid but the link flexibility is described by a full-scale 3D model that incorporates all deflections along and around x-,y-,z-axes of the three-dimensional Cartesian space. Relevant 6×6 stiffness matrix of the link may be expresses as (Connor, 1976)

$$\mathbf{K} = \frac{E}{L^3} \cdot \begin{bmatrix} A \cdot L^2 & 0 & 0 & 0 & 0 & 0 \\ 0 & 12 \cdot I_z & 0 & 0 & 0 & -6 \cdot I_z \cdot L \\ 0 & 0 & 12 \cdot I_y & 0 & 6 \cdot I_y \cdot L & 0 \\ 0 & 0 & 0 & G \cdot J \cdot L^2 / E & 0 & 0 \\ 0 & 0 & 6 \cdot I_y \cdot L & 0 & 4 \cdot I_y \cdot L^2 & 0 \\ 0 & -6 \cdot I_z \cdot L & 0 & 0 & 0 & 4 \cdot I_z \cdot L^2 \end{bmatrix} \quad (39)$$

where A, I_y, I_z are the area and the second moments of the link cross-section, J is the polar moment, E and G are the Young Coulomb modules of the link material. For a rectangular cross-section $a \times b$, the required parameters may be computed as $A = ab$ and $I_y = a^3 b / 12$, $I_z = ab^3 / 12$.

Similar to previous subsection, let apply the re-parameterization by defining the compliance with respect the z-axis as $1 / K_\theta$ (here, it is element $k_{6,6}$ of the compliant matrix $\mathbf{k} = \mathbf{K}^{-1}$). This leads to expression

$$\mathbf{k} = \frac{1}{K_\theta} \cdot \begin{bmatrix} I_z / A & 0 & 0 & 0 & 0 & 0 \\ 0 & L^2 / 3 & 0 & 0 & 0 & L / 2 \\ 0 & 0 & k_I \cdot L^2 / 3 & 0 & k_I \cdot L / 2 & 0 \\ 0 & 0 & 0 & k_J \cdot I_z / (2 \cdot L \cdot (1 + v)) & 0 & 0 \\ 0 & 0 & k_I \cdot L / 2 & 0 & k_I & 0 \\ 0 & L / 2 & 0 & 0 & 0 & 1 \end{bmatrix} \quad (40)$$

where the coefficient k_J depends on cross-section shape, $k_I = I_y / I_z$, and v is the Poisson ratio coefficient.

The kinematics of model C corresponds to the general expression $U_p R_a R_a S_p$ (see sub-section 5.1.1), it is described by the complete product of homogeneous matrices (33) that includes two passive joints $(\mathbf{q}, \mathbf{q}_t)$ incorporating five passive coordinates and three virtual-springs with 18 virtual coordinates totally (six for each link). It is obvious that analytical computation in this case is rather cumbrous, so the stiffness analysis will be performed numerically.

5.2 Stiffness analysis for model A

Let us examine first the model A that includes minimum number of flexible elements (two 1D virtual springs in the actuated joints) and may be tackled analytically. However, in spite of its simplicity, this model is potentially capable to detect the buckling phenomena at least if the initial posture of the kinematic chain is straight (S-configuration), because of evident mechanical analogy to straight columns behavior under axial compression. It is matter of research interest to evaluate other types of initial configurations with respect to the multiple loaded equilibriums, their stability and to compare with numerical results provided by the developed technique.

5.2.1 Computing static equilibriums

As follows from the kinematic equations (see subsection 5.1.2), model A includes there joint variables (q, θ_1, θ_2) one of which may be treated as a kinematically redundant one. Let us assume that the redundant variable is the passive joint coordinate q while the manipulator end-effector is located at the point $(x, y) = (3L - \delta, 0)$, where δ is a linear displacement along x-axis. Then, assuming that the initial values of the actuating coordinates (i.e. before the loading) are denotes as θ_1^0, θ_2^0, the potential energy stored in the virtual springs may be expressed as the following function of the redundant variable

$$E(q) = \frac{1}{2} K_\theta \left(\theta_1(q) - \theta_1^0 \right)^2 + \frac{1}{2} K_\theta \left(\theta_2(q) - \theta_2^0 \right)^2 \tag{41}$$

where the θ_1, θ_2 are computed via the inverse kinematics as

$$\theta_2(q) = \pm \arccos\left(\frac{(3-\Delta)^2 - 2(3-\Delta)\cos q - 1}{2} \right); \qquad \Delta = \delta / L$$

$$\theta_1(q) = \text{atan2}\left(\frac{-\sin q}{3 - \Delta - \cos q} \right) - \text{atan2}\left(\frac{2\sin \theta_2}{(3-\Delta)^2 - 2(3-\Delta)\cos q + 1} \right) - q \tag{42}$$

Using these equations, the desired equilibriums may be computed from the extrema of $E(q)$. In particular, stable equilibriums correspond to minima of this function, and unstable ones correspond to maxima:

$dE(q)/dq = 0$; $dE^2(q)/dq^2 > 0$: stable equilibrium ($E_{\min}$)

$dE(q)/dq = 0$; $dE^2(q)/dq^2 < 0$: unstable equilibrium ($E_{\max}$)

To illustrate this approach, Fig. 4 and Table 1 present a case study corresponding to the initial S-configuration of the examined kinematic chain (i.e. when $\theta_1^0 = \theta_2^0 = 0$). They allow comparing 12 different shapes of the deformated chain and selecting the best and the worst case with respect to the energy. As follows from these results, here there are two symmetrical maxima and two minima, i.e. two stable and two unstable equilibriums. Besides, the stable equilibriums correspond to Π-shaped deformated postures, and the unstable ones correspond to Z-shaped postures, as it is shown in Fig. 5. More detailed analysis allows deriving analytical expressions for the force and energy for small values of δ that will be used in the following subsection:

stable equilibrium: $\qquad E_{\min} \approx \delta \cdot K_\theta / L$; $\quad F_s \approx K_\theta / L$

unstable equilibrium: $\quad E_{\max} \approx \delta \cdot 3 K_\theta / L$; $\quad F_s \approx 3 K_\theta / L$

It worth also mentioning that only stable equilibriums may be observed in practice and only this type of solutions is produced by the algorithm proposed in Section 3.

Configuration	q	θ_1	θ_2	Potential Energy	Configuration for stable static equilibrium
	$-\varphi_5$	φ_2	0	$1.5\dfrac{K_\theta}{L}$	
	$-\varphi_1$	φ_1	φ_1	$1.0\dfrac{K_\theta}{L}$	
	$-\varphi_4$	0	φ_2	$1.5\dfrac{K_\theta}{L}$	
	0	$-\varphi_1$	$-\varphi_3$	$2.5\dfrac{K_\theta}{L}$	
	φ_4	$-\varphi_2$	φ_2	$3.0\dfrac{K_\theta}{L}$	
	φ_1	$-\varphi_3$	φ_1	$2.5\dfrac{K_\theta}{L}$	
	φ_5	$-\varphi_2$	0	$1.5\dfrac{K_\theta}{L}$	
	φ_1	$-\varphi_1$	$-\varphi_1$	$1.0\dfrac{K_\theta}{L}$	
	φ_4	0	$-\varphi_2$	$1.5\dfrac{K_\theta}{L}$	
	0	φ_1	$-\varphi_3$	$2.5\dfrac{K_\theta}{L}$	
	$-\varphi_4$	φ_2	$-\varphi_2$	$3.0\dfrac{K_\theta}{L}$	
	$-\varphi_1$	$-\varphi_3$	$-\varphi_1$	$2.5\dfrac{K_\theta}{L}$	

$$\varphi_1 = \arccos(1 - \tfrac{1}{2}\Delta) \; ; \; \varphi_2 = \arccos(1 - \tfrac{3}{2}\Delta + \tfrac{1}{4}\Delta^2) \; ; \; \varphi_3 = \arccos(1 - 2\Delta + \tfrac{1}{4}\Delta^2) \; ;$$

$$\varphi_4 = \arccos\left(\frac{12 - 6\Delta + \Delta^2}{4(3 - \Delta)}\right) \; ; \; \varphi_5 = \arccos\left(\frac{6 - 6\Delta + \Delta^2}{2(3 - \Delta)}\right)$$

Table 1. Selected postures of the deformed kinematic chain and their corresponding equilibriums (case of unloaded S-configuration, $\delta = L/10$)

Thank You for previewing this eBook

You can read the full version of this eBook in different formats:

- ➢ HTML (Free /Available to everyone)

- ➢ PDF / TXT (Available to V.I.P. members. Free Standard members can access up to 5 PDF/TXT eBooks per month each month)

- ➢ Epub & Mobipocket (Exclusive to V.I.P. members)

To download this full book, simply select the format you desire below